Chemical Engineering Journal 168 (2011) 1331–1345

Contents lists available at ScienceDirect

Chemical Engineering Journal

journal homepage: www.elsevier.com/locate/cej

Theory of flow distribution in manifolds

Junye Wang*

Sustainable Soils and Grassland Systems Department, Rothamsted Research, North Wyke, Okehampton, Devon EX20 2SB, UK

ARTICLE INFO

Article history:
Received 8 November 2010
Received in revised form 8 January 2011
Accepted 20 February 2011

Keywords:
Flow distribution
Distributor
Parallel channels
Manifold
Spargers
Maldistribution

ABSTRACT

Flows in manifolds are of great importance in quite diverse fields of science and technology, including fuel cells, spargers, solar collectors, microchannels, porous infiltration and irrigation. Theory of flow distribution and pressure drop is vital to predict process performance and efficiency of manifold systems. In this paper, we examined research and development of theoretical models and methodology of solutions in flow in manifolds and highlight remarkable advances in the past fifty years. The main existing models and solution methods were unified further to one theoretical framework, including Bernoulli theory and momentum theory, and discrete and continuum methodologies. The generalised model was applicable to not only designs of continuum manifolds but also those of discrete manifolds with constant or varying factors. The procedure of design calculation is in reality straightforward without requirements of iteration, successive approximation and computer programme. The theoretical model provides easy-to-use design guidance to investigate the interactions among structures, operating conditions and manufacturing tolerance under a wide variety of combination of flow conditions and geometries through three general characteristic parameters (E, M and ζ) and to minimize the impact on manifold operability.

1. Introduction

The flow in manifold systems is extensively encountered in many industrial processes including chemical [1–3], biomedical [4,5], mechanical [6–8] and civil and environmental engineering [9–11]. The uniformity of the flow distribution in a manifold system often determines efficiency, durability and cost of the units of the chemical and biological processes. There are two common structures of manifolds used for flow distributions: consecutive [1–11] and bifurcation [12,13].

A fractal bifurcation structure assumes that the fluid behaves tree-like where the channels at the last level have the smallest length and diameter, in the bifurcation structure (Fig. 1a) the reaction channels (last level channels) are usually the longest. The bifurcation structure is generally a good design in the absence of channel dimensional variations. It is the only one where flow distribution does not change for different flow rates at high Re. However, the equipartition is greatly depending on manufacturing tolerance and port blockage. Furthermore, when a large number of ports, a large pressure drop is expected due to turning loss and it is also more complex to design and fabricate. Therefore, it is unsuitable for those cases where additional pressure losses become important.

A consecutive manifold consists of multiple ports/holes with constant cross-sectional area as shown in Fig. 1b. In a consecutive manifold the main fluid stream entrances a manifold and branches continuously along the manifold. This type of manifolds is the most commonly used flow distributors due to their clear advantages of simplicity and less pressure drop over bifurcation structures. This means the greatest potential to reduce development and manufacturing cost and accelerate design and manufacturing cycle. However, using a consecutive manifold, a key question which arises in the design of such units is a possibility of the severe flow maldistribution problems. Some ports may be starved of fluids, while others may have them in excess, which reduces system performance and efficiency. It is a key to predict the performance and efficiency of various manifold configurations so that high efficiency and cost reduction can be achieved through an optimal geometrical structure. This paper will focus on theory of flow in consecutive manifolds due to a wide range of applications. There are three approaches to study pressure drop and flow distribution in a manifold: computational fluid dynamics (CFD) [14–19], discrete models [7,20] and analytical models [2,21,22].

The CFD is a somewhat detailed approach in which modelling has potential to resolve real-world 3-D engineering structures. The pressure drop and flow distribution can be predicted using this approach without the knowledge of flow coefficients, such as the friction and pressure recovery coefficients. However, the CFD is unsuitable for optimizing manifold geometry and preliminary designs since it is expensive to generate the computational geometry and mesh for each new configuration. Furthermore, there are still the difficulties for the turbulence models and the boundary models associated with solving swirling or curvature flows because

* Tel.: +44 1837883552; fax: +44 183782139.
E-mail address: junye.wang@bbsrc.ac.uk

1385-8947/$ – see front matter © 2011 Elsevier B.V. All rights reserved.
doi:10.1016/j.cej.2011.02.050

Nomenclature

A	constant in Eq. (A5) (= $3Q$)
B	constant in Eq. (21), defined by Eq. (A7)
C	constant in Eq. (5)
C_1, C_2	undetermined constant in Eq. (22)
C_f	coefficients of turning losses
d, d_{ch}	diameter and hydraulic diameter of the ports (m)
D, D_h	diameter and hydraulic diameter of manifold (m)
f	friction factor
E	Ratio of manifold length to diameter (L/D)
F, F_c	cross-sectional area of manifold and port (m^2)
J	constant in Eq. (21), defined by Eq. (A11)
k	pressure recovery factor (=$(2-\beta)/2$)
l_c	length of port
L	length of manifold (m)
M	ratio of sum of all the port areas to area of manifold ($F_c n/F$)
n	numbers of ports
n_c	threshold number of ports
p	dimensionless pressure defined by Eq. (13)
p_c	dimensionless ambient pressure
$\bar{p}$	dimensionless pressure defined by Eq. (6)
P	pressure in manifold
P_c	ambient pressure
Q	coefficient in Eq. (19), defined by Eq. (17)
r, r_1, r_2	roots of characteristic equation
R	coefficient in Eq. (19), defined by Eq. (18)
u_c	dimensionless port velocity defined by Eq. (13)
U_c	port velocity (m/s)
$\bar{U}$	dimensionless velocity defined by Eq. (6) in manifold
v_c	dimensionless volume flow rate in ports
w	dimensionless velocity defined by Eq. (13) in manifold
W	velocity in manifold (m/s)
x	dimensionless axial coordinate defined by Eq. (13) in manifold
X	(m)
y	axial coordinate defined by Eq. (6) in manifold

Greek symbols

α	constant in Eq. (33)
β	average velocity ratio in manifold (W_c/W)
γ	constant in Eq. (33)
ρ	fluid density (kg/m^3)
τ	wall shear stress (N/m^2)
ζ	average total head loss coefficient for port flow
ξ	coefficient of non-smooth ducts

Subscripts

i	the *ith* section in manifold
0	the inlet of a manifold

the eddy-viscosity models failed to capture the anisotropy of strain and Reynolds stresses under the action of Coriolis and centrifugal forces [23–26].

Discrete model is also called network model. In a discrete model, a manifold is represented as a network of multiple-junctions traversed by the fluid flow. Then, mass and momentum conservation equations can be built at each junction. Finally, a set of difference equations is solved using an iteration program. Because of its relatively simplicity this approach has been used by many researchers [19,20]. However, a designer cannot use its results directly since this approach usually needs computer programme. It is still inconvenient for the preliminary design and optimisation of the manifold structures since there are no explicit relation between flow performance and manifold geometries.

Analytical model is also called the continuous model in which flow is considered to be continuously branched along a manifold. It has been shown intuitively, as well as mathematically, that the continuous manifolds are limiting cases of the discrete manifolds [2,28,29]. In mathematical viewpoint, the fluid mechanical principles in a continuous manifold lead to a differential rather than a difference equation in a discrete one. Furthermore, an explicit analytical solution can directly be converted to one solution of discrete systems. For these reasons, the continuous models are also fundamentals of various discrete models.

A main advantage of analytical models over the CFD and the discrete models is that it is simple and flexible for manifold designers since solutions based on the differential equation can be represented more simply and compactly than is the case for calculations using the non-linear difference equations. Furthermore, a generalised analytical model has unique possibility to correlate explicitly the performance, such as flow distribution and pressure drop, and manifold structures, such as diameters and shape, pitch and duct lengths. Particularly, for preliminary design, we have less information if a geometrical structure is optimal but major decisions should be made in this stage, such as cost, durability, maintenance and performance. The rational yet tractable generalised model offers possibility to explore flow performance under various geometries of manifolds.

Due to these clear advantages, analytical solutions have received fairly good attentions in the past fifty years. There are diverse models for flow distributions in manifolds which scatter in different fields. Most of the theoretical models are traditionally based on Bernoulli theorem or slight modification thereof. However, a problem raised from the experiments by McNown [30] and Acrivos et al. [31]. Their experimental results showed that there was a pressure rise after flow branching as shown in Fig. 2. This phenomenon was explained by Wang et al. [2,27–29]. Because the lower energy fluid in the boundary layer branches through the channels the higher energy fluid in the pipe centre remains in the pipe. So the average specific energies in a cross-section will be higher in the downstream than in the upstream. Since energy balance is based on the average value in the cross-section, these higher specific energies cannot be corrected and lead to an error. Hence, according to the First Law of Thermodynamics, when the specific mechanical energies are multiplied by the relevant mass flow rate terms, the mechanical energy after branching for the manifold can apparently be greater than the approaching energy. Thus, it is not surprising that a pressure rise was predicted by Bernoulli theorem, which has been observed by the experiment. Recent researchers preferred to apply momentum conservation along a manifold to avoid this problem [2,6,22,27–29]. The advantage of applying the momentum conservation is that one does not need to know detailed flow patterns and the flow process can be simplified. Any error due to simplification can be corrected with pressure recovery factor, friction factor and discharge factor.

Since both Bernoulli and momentum theory are used to describe flow in manifolds they should be identical in all the fields. In practice, there are a wide range of models in the different fields. There is much ambiguity what difference between them. Wang [27,28] did the first attempt to unify main theoretical models into one theoretical framework. He demonstrated that Bernoulli equation was just a special case of the momentum model. In this regard, a fruitfully unified perspective is now emerging—one quite natural to chemical engineers. However, there are still key issues in this field. For example, is the theory developed by Wang applicable to arbitrary shape and varying factors? Furthermore, many models on modified Bernoulli equation seem to have similar formula as those on

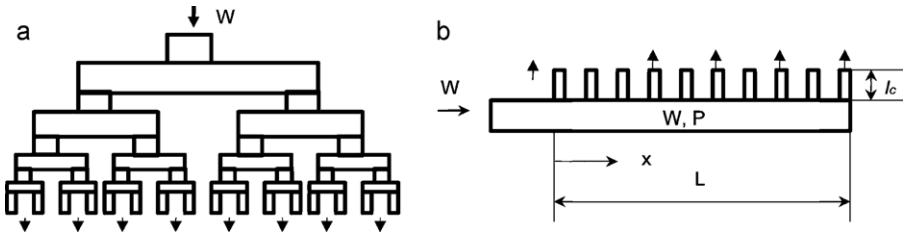

Fig. 1. Schematic diagram of manifold: (a) bifurcation and (b) consecutive.

the momentum. For example, the theoretical model developed by Acrivos et al. [31] was very similar to those on the momentum theory. Therefore, there is still ambiguity which theoretical model is the most generalised in this area [18,32]. What measurable progresses have been made in this field in the past fifty years? It is desirable to perform a deeper examination of flow modelling in manifold systems. Wang's work [27,28] will allow us to stimulate further activity about these key issues along this promising path.

The primary aim of this paper is to extend Wang's model for applications of varying factors and arbitrary shape distributor following Wang's previous work [27,28]. We will demonstrate that Wang's model is applicable to those under varying the friction and the pressure recovery factors if using section by section substitution and is suitable for arbitrary shape of cross-section if using hydraulic diameter and wetted perimeter. The second aim is to continue to unify existing models and methodologies, and to clarify ambiguity in this area. We will demonstrate that the present model is fundamentals of flow in various manifolds and is applicable to designs of both continuum and discrete manifolds. In following section, we revisit developments of theoretical models of flow in manifolds. Then we will build the coupling equation between the velocity and pressure and re-examine the solution methodologies of the theoretical models in the past fifty years and highlight remarkable advances. The applicability of the analytical solutions to varying factors will be arranged in Section 5. The results and discussion will be in Section 6. In the last section, some concluding remarks are given.

2. Theoretical models

To predict the pressure rise phenomena, Acrivos et al. [31] modified empirically Bernoulli equation by adding a correction term of momentum. Using a slight modification of friction factor on Blasius law ($F = F_0\bar{U}^{-1/4}$), they derived a normalised governing equation as following (for notional convenience, $\bar{U}$ and $\bar{p}$ replace U and P, respectively) (Eq. (1.14) of Ref. [31]):

$$\frac{d\bar{p}}{dy} + \bar{U}\frac{d\bar{U}}{dy} + F_0\bar{U}^{7/4} = 0 \quad (1)$$

where $\bar{U}$, $\bar{p}$ and y were normalised axial velocity, pressure and coordinate of manifold, respectively, and F_0 was a combination of friction factor and momentum recovery factor.

Kulkarni et al. [18,32] stated that this model was the most generalised in the absence of clear indications. If Kulkarni et al.'s statement was correct, that would mean that our advances in this area were nothing in the past fifty years. Let's re-examine the model developed by Acrivos et al. There were three key limitations while this model introduced the pressure recovery factor, k, for the first time. Firstly it was empirical modification of Bernoulli equation. F_0 was a combination of the friction and the pressure recovery factors so that it was difficult to analyse the separated effects of friction and momentum and to explain their interactions. It was also impossible to distinguish flow regions theoretically. Secondly, they assumed the friction factor was varying with fluid velocity to the power of $-1/4$. This limited applicability of the model only in Blasius' flow, namely, a range of Reynolds number ($2200 < \mathrm{Re} < 10^5$). Since flow was not always in this region, this model was not most generalised. Finally, they did not obtain an analytical solution even in this specific Reynolds number. Thus, they had to use graphs or tables to present relationship between geometries and flow conditions. This was incomplete for a wide range of geometrical structures. It was also difficult to have a whole picture of flow in manifolds. In addition, it was inconvenient for a designer to use it in preliminary design in which we had less information if a geometrical structure was optimal but major decisions should be made in this stage.

These limitations inspired huge efforts in the past fifty years. Bajura [6] developed the first general theoretical model for flow distribution in manifolds based on mass and momentum conservation in which a direct physical definition of the pressure recovery factor was given. His model was extended by Bassiouny and Martin [22] into plate heat exchanger. Wang et al. [2,29] extended further their model for design of distributors. Since then, flow in dividing manifolds was formulated as a current standard equation, a second order nonlinear ordinary differential equation as follows in Ref. [2,22,27–29]):

$$\frac{1}{\rho}\frac{dP}{dX} + \frac{f}{2D}W^2 + (2-\beta)W\frac{dW}{dX} = 0 \quad (2)$$

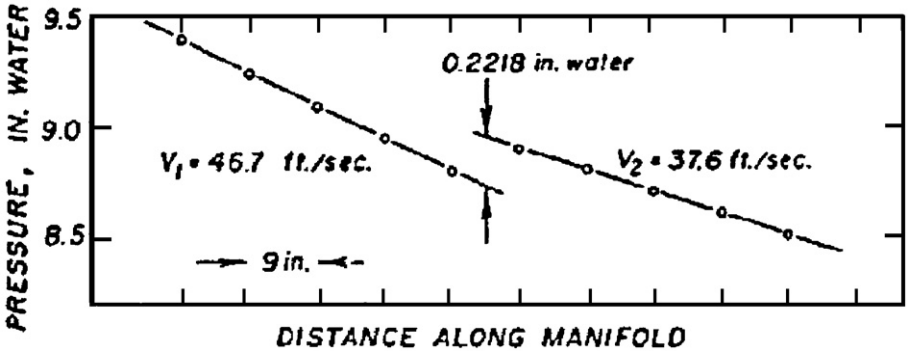

Fig. 2. Typical pressure rise phenomena observed near a single outlet port [31].

In Eq. (2) if (2 – β) is replaced by 2*k*, one obtain another formula [2]:

$$\frac{1}{\rho}\frac{dP}{dX} + \frac{f}{2D}W^2 + 2kW\frac{dW}{dX} = 0 \tag{3}$$

where *k* is pressure recovery factor.

It is clear that Eq. (2) was derived completely based on the first principle of mass and momentum conservation. The value $\beta = 0$implies that the flow leaves the manifold at right angles (i.e., axial component of the velocity is equal to zero) and represents the maximum possible static pressure recovery. The value $\beta = 1$ implies that the fluid would leave the manifold without losing any axial momentum. Wang [27,28] rearranged Eq. (2) as follows:

$$\frac{1}{\rho}\frac{dP}{dX} + \frac{f}{2D}W^2 + \frac{2-\beta}{2}\frac{dW^2}{dX} = 0 \tag{4a}$$

or to a discrete equation:

$$\Delta P + \frac{\rho f}{2D}W^2\Delta X + \frac{(2-\beta)\rho}{2}\Delta W^2 = 0 \tag{4b}$$

Eq. (4b) is a fundamental equation for most of discrete models. It is clear that Eq. (4a) is limiting case of Eq. (4b) when $\Delta X \to 0$. The discrete model has the same origin as the analytical one. Therefore, an analytical model is a limited version of a discrete model. It should be noted that the friction and the pressure recovery factors were not limited to be constants in Eqs. (2–4). On the other hand, Eq. (4a) can be simplified to Bernoulli equation without the potential energy term when$\beta = 1$. Therefore, Bernoulli equation is just a special case of Eq. (4). Moreover, Eq. (3) can be simplified to Eq. (1) with slight adjustments after substituting Blasius' equation, $f = 0.3164/\mathrm{Re}^{0.25} = f_0 W^{-1/4}$, as follows.

$$\frac{1}{\rho(2kW_0^2)}\frac{dP}{((4\alpha C/D)\sqrt{2k})dX} + \frac{f}{2k2W_0^2(4\alpha C\sqrt{2k})}W^2 + \frac{1}{W_0^2}\frac{WdW}{((4\alpha C/D)\sqrt{2k})dX} = 0$$

The readers can refer to Ref. [31] for the physical definitions of the constants, *C* and α in the above equation.

$$\frac{d\bar{p}}{dy} + \frac{f}{2k2(4\alpha C\sqrt{2k})}\bar{U}^2 + \bar{U}\frac{d\bar{U}}{dy} = 0 \tag{5a}$$

Substituting the law of Blasius $f = f_0\bar{U}^{-1/4}$ into Eq. (5a), $\frac{d\bar{p}}{dy} + \frac{f_0}{2^{5/2}k^{3/2}\alpha C}\bar{U}^{7/4} + \bar{U}\frac{d\bar{U}}{dy} = 0$

$$\frac{d\bar{p}}{dy} + \bar{U}\frac{d\bar{U}}{dy} + F_0\bar{U}^{7/4} = 0 \tag{5b}$$

where $F_0 = \dfrac{f_0}{2^{5/2}k^{3/2}\alpha C}$, $\bar{p} = \dfrac{P}{\rho(2kW_0^2)}$, $\bar{U} = \dfrac{W}{W_0}$ and

$$y = \left(\frac{4\alpha C}{D}\sqrt{2k}\right)X \tag{6}$$

Eq. (5b) is the same one of Eq. (1). It was clear that Eq. (1) was limited in Blasius flow and was not suitable for other flows, such as laminar flow in which *f* was formulised by Poiseuille's equation, $f = 64/\mathrm{Re} = f_0 W$. Unlike Eq. (1), Eq. (3) is not limited in Blasius flow and *f* can be any function of velocity, including Blasius flow. Therefore, Eq. (1) is just a special case of Eq. (3) when $f = 0.3164/\mathrm{Re}^{0.25} = f_0 W^{-1/4}$. Eq. (3) is the most generalised model of flow in manifolds since it has overcome the first two limitations of Acrivos et al.'s.

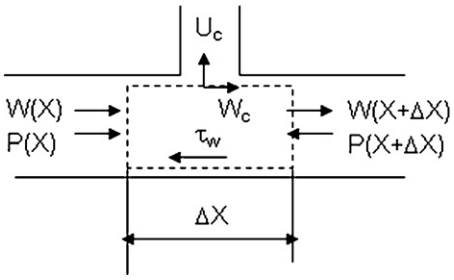

Fig. 3. Control volume for the manifold.

3. Coupling of velocity and pressure in theoretical models

It has been desirable to solve analytically Eq. (2) or Eq. (3) since an explicit relation can fully explore interaction between flow performance and manifold structure. Before an analytical solution of Eq. (3), it is necessary to couple velocity and pressure. We follow our previous work [27,28] here for the sake of self-contained papers and for later use. We will show that the governing equation of flow in distributors possesses the same mathematical style as that in the U-type arrangement.

The control volume in a dividing manifold is shown in Fig. 3. The mass and momentum balances can be written as follows:

3.1. Mass conservation

$$\rho FW = \rho F\left(W + \frac{dW}{dX}\Delta X\right) + \rho F_c U_c \tag{7}$$

where *F* and F_c are the cross-sectional areas of the manifold and the port, respectively, *W* the axial velocity in manifold, U_c the port velocity, *X* axial coordinate in the intake header, and ρ fluid density. Setting $\Delta X = L/n$, *n* is the number of ports and *L* length of the manifold.

$$U_c = -\frac{FL}{F_c n}\frac{dW}{dX} \tag{8}$$

3.2. Momentum conservation

$$PF - \left(P + \frac{dP}{dX}\Delta X\right)F - \tau_w P_h \Delta X = \rho F\left(W + \frac{dW}{dX}\Delta X\right)^2 - \rho FW^2 + \rho F_c U_c W_c \tag{9}$$

where *P* is pressure in the manifold, P_h is wetted perimeter, $W_c = \beta W$ and τ_w is given by Darcy–Weisbach formula, $\tau_w = f\rho(W^2/8)$ for any cross sectional manifold.

After inserting τ_w and W_c into Eq. (9) and neglecting the higher orders of ΔX, Eq. (9) can be rearranged as follows:

$$-F\frac{dP}{dX}\Delta X - \rho f\frac{W^2}{8}P_h\Delta X = \rho F2W\frac{dW}{dX}\Delta X - \rho\beta\frac{FL}{n}W\frac{dW}{dX}$$

$$\frac{1}{\rho}\frac{dP}{dX} + \frac{f}{2}\frac{P_h}{4F}W^2 + (2-\beta)W\frac{dW}{dX} = 0$$

$$\frac{1}{\rho}\frac{dP}{dX} + \frac{f}{2D_h}W^2 + (2-\beta)W\frac{dW}{dX} = 0 \tag{10}$$

where D_h is hydraulic diameter. $D_h = 2ab/(a+b)$ for rectangular shape, and *a* and *b* are width and height of the cross-section of the rectangular manifold, respectively. Thus, Eq. (10) is suitable for any shape.

The flow through ports can be described by Bernoulli's equation with a consideration of flow turning loss. Hence, the velocity

in a port, U_c, is correlated to the pressure difference between the manifold and the ambient as follows:

$$P - P_c = \rho\left(1 + C_f + f_c\frac{l_c}{d_{ch}}\right)\frac{U_c^2}{2} = \rho\zeta\frac{U_c^2}{2} \tag{11}$$

where C_f is coefficient of turning loss from the manifold into the ports, l_c is length of the ports, d_{ch} is hydraulic diameter of port and f_c is the friction coefficient for the port flow.

Inserting Eq. (8) into Eq. (11), gives:

$$P - P_c = \frac{1}{2}\rho\zeta\left(\frac{FL}{F_c n}\right)^2\left(\frac{dW}{dX}\right)^2 \tag{12}$$

Eqs. (10) and (12) can be reduced to dimensionless form using the following dimensionless groups.

$$p = \frac{P}{\rho W_0^2}, \quad p_c = \frac{P_c}{\rho W_0^2}, \quad w = \frac{W}{W_0}, \quad u_c = \frac{U_c}{W_0}, \quad x = \frac{X}{L} \tag{13}$$

where W_0 is the inlet velocity of the manifold.

$$\frac{dp}{dx} + \frac{fL}{2D_h}w^2 + (2-\beta)w\frac{dw}{dx} = 0 \tag{14}$$

$$p - p_c = \frac{1}{2}\zeta\left(\frac{F}{F_c n}\right)^2\left(\frac{dw}{dx}\right)^2 \tag{15}$$

Inserting Eq. (15) into Eq. (14) and after rearranging, one obtains an ordinary differential equation for the velocity in the distributor:

$$\frac{dw}{dx}\frac{d^2w}{dx^2} + \frac{2-\beta}{\zeta}\left(\frac{F_c n}{F}\right)^2 w\frac{dw}{dx} + \frac{fL}{2D_h\zeta}\left(\frac{F_c n}{F}\right)^2 w^2 = 0 \tag{16a}$$

Similarly, we can derive the governing equation of flow in combining manifolds as follows [27],

$$\frac{dw}{dx}\frac{d^2w}{dx^2} + \frac{2-\beta}{\zeta}\left(\frac{F_c n}{F}\right)^2 w\frac{dw}{dx} - \frac{fL}{2D_h\zeta}\left(\frac{F_c n}{F}\right)^2 w^2 = 0 \tag{16b}$$

Eqs. (16a) and (16b) are second order nonlinear ordinary differential equations and are the standard formula for dividing and combining flow in manifold. The second term in the left hand of Eq. (16) represents a momentum contribution known as the momentum term, and the third term does the friction contribution as the friction term.

We define two constants:

$$Q = \frac{2-\beta}{3\zeta}\left(\frac{F_c n}{F}\right)^2 \tag{17}$$

$$R = -\frac{fL}{4D_h\zeta}\left(\frac{F_c n}{F}\right)^2 \tag{18}$$

Thus, Eq. (16) is reduced as follows:

$$\frac{dw}{dx}\frac{d^2w}{dx^2} + 3Qw\frac{dw}{dx} - 2Rw^2 = 0 \tag{19}$$

Similarly, the combing flow as follows,

$$\frac{dw}{dx}\frac{d^2w}{dx^2} + 3Qw\frac{dw}{dx} + 2Rw^2 = 0 \tag{20}$$

Eq. (19) is mathematically identical to that of U-type [27]. Now we have proved that Eq. (2) can be used for arbitrary shape of cross-section after uses hydraulic diameter and wetted perimeter. Furthermore, Eqs. (19) and (20) are no any limitation of the constant factors or varying ones. Therefore, these two equations are most generalised model of flow in the dividing and combining manifolds, respectively.

4. Analytical solution

4.1. Previous solutions

Without loss of generality, we take Eq. (19) as example to illustrate theoretical solutions of flow in dividing manifolds hereafter. Eq. (19) is the most generalized governing equation of the dividing flow distribution. However, it has been a well-known challenge in the field of flow in manifold systems to find its general solution. Ones had to resort to numerical computation because of complexity of coupling pressure and velocity and nonlinearity [1,31]. On the other hand, researchers simplified the model and neglected terms of the models or assumed a flow distribution despite this might cause a significant error.

The equations were solved by Bajura [6] and Bassiouny and Martin [22] after neglecting friction effect. Therefore, their solutions were only validated for a short manifold. Bassiouny and Martin derived a characteristic parameter to determine flow regions. Since then, their solutions were extensively used by the following researchers.

Kee et al. [33] and Maharudrayya et al. [34], on the other hand, retained the frictional term in their model equation but the inertial term was neglected totally. Thus, it is clear that Maharudrayya et al.'s model function at an extreme case of Eq. (16) when $\beta = 0$ while Bernoulli equation at its another end case when $\beta = 1$. Wang [28,35] indicated that the neglecting of the inertial terms will lose two solutions with the triangular function and the exponent function. Furthermore, the phenomena of pressure rise cannot be captured because there is no flow branching effect. The neglecting of inertial term may cause an error of 20–50% since β was at of order of 0.5–1.

Wang et al. [2,8,29] assumed a velocity profile to solve analytically Eq. (3). Their results showed that there were three regions: momentum dominant, momentum-friction reciprocity and friction dominant regions. A quantitative characteristic parameter was used to determine the flow behaviour and the flow regions. Wang et al. [2,29] also summarised the effect of manifold structure on the friction and the pressure recovery factors. The friction factor was dependent on three ratios: the channel diameter to the header diameter, the spacing length to the header diameter, and the sum of the areas of all the channels to the cross-sectional area of header. They also formularised theoretically the pressure recovery factor k, in a manifold ($k = \alpha + 2\gamma\ln(W/W_0)$).

Wang et al. [2] carried out successfully the first attempt to solve analytically Eq. (3) under variation of both friction and pressure recovery factors. They took all the flow regions of Reynolds number into account and allowed the value of both f and k to vary along the pipe according to the local velocity. Here Kulkarni et al. [18] might misunderstand that the solutions of Wang et al.'s were under assumption of constant friction factor. They considered the variation of f along the pipe was a major limitation of Wang's model. Furthermore, Wang et al. [36] corrected the assumption of linear velocity profile using a power velocity profile instead.

Despite the solutions of Wang et al.'s were under an ideal assumption of linear velocity profiles, these solutions are extremely useful for determining the possibility of uniform flow distribution for a given geometry of a distributor. Their explicit solutions have a direct and explicit relationship between geometries and flow performance. Therefore, their work proved theoretically interaction between the friction and the momentum in a distributor and derived a characteristic parameter to determine flow regions. Of course, the assumption of velocity profiles did restrain its applications. In contrast Acrivos et al.'s numerical solution, however, had to define $dw/dx = -M_0$ (a linear velocity assumption) (Eq. (1.24) of Ref. [31]) to analyse their results. Due to an inherent limitation, numerical methodology could not obtain direct relation between flow

performance and manifold structure. They had to employ graphs to present relationship between geometry and flow conditions. Therefore, this limited the solution application in the preliminary design.

Chou and Lei [9] carried out an attempt to solve analytically Bajura's model using an alternative variable of discharge flow which converted the second order Bajura's equation to the first order differential equation. Thus, they derived an analytical solution of the discharge flow distribution for dividing manifold. Unfornunately, they did not solve completely Bajura's equation and obtained velocity distribution and pressure drop along manifold.

In the recent years, Wang [27,28] obtained successfully the general solutions of the governing equation (19) for flow distribution in U- and Z-type manifold for the first time without any drop of the friction and the momentum term. His recent work allows us to start an exciting new approach into flow in distributors and to offer a real step forward in understanding of flow in manifold systems.

4.2. Solution procedure

The analysis for the dividing manifold is similar to that of the U-type done by Wang [27,28]. The interested reader can refer to Appendix A for the details of the solution of Eq. (19).

Here we take a complex characteristic roots (Eq. (A13)):

$$\begin{cases} r = B \\ r_1 = -\dfrac{1}{2}B + \dfrac{1}{2}i\sqrt{3}J \\ r_2 = -\dfrac{1}{2}B - \dfrac{1}{2}i\sqrt{3}J \end{cases} \tag{21}$$

where B and J are given in Eqs. (A7) and (A11), respectively.

Thus, we have two set of solutions of Eq. (21), $r = \beta$ represents a case of no fluid flow in the manifold. The solutions of Eq. (21) depends on the sign of $Q^3 + R^2$, which has three cases. The complex root appears explicitly while r_1 and r_2 do, but this does not say anything about the number of real and complex roots since $\sqrt{Q^3 + R^2}$ are themselves, in general, complex. However, determining which roots are real and which are complex can be accomplished by noting that if the polynomial discriminant $Q^3 + R^2 > 0$, one root is real and two are complex conjugates; if $Q^3 + R^2 = 0$, all roots are real and at least two are equal; and if $Q^3 + R^2 > 0$, all roots are real and unequal.

However, the case of $R^3 + Q^2 < 0$ is impossible in practical situation for the dividing flow in manifolds because Q is greater than (or equal to) zero. $R^3 + Q^2 = 0$ is an extreme case when $F \gg nF_c$ or $\zeta \to \infty$. So we take only $R^3 + Q^2 > 0$ for analysis and discussion. Some details are given in Appendix B for $R^2 + Q^3 < 0$ and $R^2 + Q^3 = 0$.

Two conjugated solutions retain the same as Eq. (21):

$$r_1 = -\frac{1}{2}B + \frac{1}{2}i\sqrt{3}J$$
$$r_2 = -\frac{1}{2}B - \frac{1}{2}i\sqrt{3}J$$

Thus, the general solution of Eq. (19) and boundary conditions can be written as follows:

$$\begin{aligned} &w = e^{-Bx/2}\left[C_1\cos(\sqrt{3}Jx/2) + C_2\sin(\sqrt{3}Jx/2)\right] \\ &w = 0, \quad \text{at} \quad x = 1 \\ &w = 1, \quad \text{at} \quad x = 0 \end{aligned} \tag{22}$$

Axial velocity in the manifold:

$$w = e^{-Bx/2}\left[\frac{\sin(\sqrt{3}J(1-x)/2)}{\sin(\sqrt{3}J/2)}\right] \tag{23}$$

Port velocity by substituting Eq. (23) into Eq. (8):

$$u_c = \left(\frac{F}{2nF_c}\right)e^{-Bx/2}\left[\frac{B\sin(\sqrt{3}J(1-x)/2) + \sqrt{3}J\cos(\sqrt{3}J(1-x)/2)}{\sin(\sqrt{3}J/2)}\right] \tag{24}$$

Flow distribution using Eq. (24):

$$\begin{aligned} v_c &= \frac{F_c U_c}{FW_0/n} = \left(\frac{nF_c}{F}\right)u_c \\ &= \frac{1}{2}e^{-Bx/2}\left[\frac{B\sin(\sqrt{3}J(1-x)/2) + \sqrt{3}J\cos(\sqrt{3}J(1-x)/2)}{\sin(\sqrt{3}J/2)}\right] \end{aligned} \tag{25}$$

Pressure drop in the ports after substituting Eq. (23) into Eq. (15):

$$p - p_c = \left(\frac{\zeta}{2}\right)\left(\frac{F}{nF_c}\right)^2 e^{-Bx}\left[\frac{B\sin(\sqrt{3}J(1-x)/2) + \sqrt{3}J\cos(\sqrt{3}J(1-x)/2)}{2\sin(\sqrt{3}J/2)}\right]^2 \tag{26}$$

Pressure drop in the manifold after substituting Eq. (23) into Eq. (14) and integrating Eq. (14):

$$\begin{aligned} p - p_0 = {} & \frac{Lf}{4D_h B\sin^2(\sqrt{3}J/2)}\left(e^{-Bx} - 1\right) - \frac{Lf}{4D_h(B^2 + 3J^2)\sin^2(\sqrt{3}J/2)} \\ & \{Be^{-Bx}\cos[\sqrt{3}J(1-x)] - \sqrt{3}Je^{-Bx}\sin[\sqrt{3}J(1-x)] + B\cos(\sqrt{3}J) + \sqrt{3}J\sin(\sqrt{3}J)\} \\ & - \frac{2-\beta}{2}\frac{e^{-Bx}\sin^2[\sqrt{3}J(1-x)/2]}{\sin^2(\sqrt{3}J/2)} \end{aligned} \tag{27}$$

5. Applicability of the analytical solutions to varying friction and pressure recovery factors

Though Eq. (19) is solved under the assumptions of the constant friction and the constant pressure recovery factors, its analytical solutions can still be used for varying factors as well as discrete manifolds. This is justified because Eq. (19) is derived in a control volume or a T junction. That means that it is valid not only for the whole manifold but also for each section or junction. Of course, its solutions are valid for each section as well.

Thanks for the fully explicit solutions; it makes it easy to calculate flow distribution and pressure drop in a discrete manifold along the manifold because we can calculate them section by section using the present analytical solutions. Since the local friction and the pressure recovery factors can be functions of the local velocity, they can be calculated using the local velocity at each section of the manifold. A section by section solution allows also varying factors along the manifold. This demonstrates why the continuous models are fundamentals of various discrete models and an explicit analytical solution can directly be used to one of discrete manifolds.

Without loss of generality we transfer the continuum solutions into discrete one for the $(i+1)$th section. after derive Q_i and R_i using the local friction and pressure recovery factors for the ith section. Analytical solutions can be substituted through section by section difference equations.

5.1. Flow coefficients

A systematic analysis of the friction factors and the pressure recovery factors has been performed by Wang et al. [2]. A general expression of the friction factor can be given:

$$f_i = \xi f_i' = \xi f(\mathrm{Re}) \tag{28}$$

Here we take circular manifold as an example to illustrate the solution procedure and $\xi = 1$ for the sake of simplicity. Inserting Eq. (28) into Eq. (18), one obtains R_i for the ith section,

$$R_i = -\frac{f_i L}{4D_h\zeta_i}\left(\frac{F_c n}{F}\right)^2 \tag{29}$$

when $\mathrm{Re} < 2200$, $f_i = 64/\mathrm{Re}_i$

$$\begin{aligned} R_i &= -\frac{16\nu L}{D_h^2\zeta W_i}\left(\frac{F_c n}{F}\right)^2 = -\frac{16(L/D_h)}{(W_0 D_h/\nu)\,\zeta(W_i/W_0)}\left(\frac{F_c n}{F}\right)^2 \\ &= -\frac{16E}{Re_0\zeta w_i}M^2 \end{aligned} \tag{30}$$

where $M = F_c n/F$ and $E = L/D_h$

When $2200 < Re < 10^5$, $f_i = 0.3164/Re_i^{0.25}$.

$$R_i = -\frac{f_i L}{4D_h\zeta}\left(\frac{F_c n}{F}\right)^2 = -\frac{0.3164(L/D_h)}{4(W_0 D_h/\nu)^{0.25}\zeta(W_i/W_0)^{0.25}}\left(\frac{F_c n}{F}\right)^2 = -\frac{0.0791E}{Re_0^{0.25}\zeta w_i^{0.25}}M^2 \quad (31)$$

When $Re > 10^5$, $f(Re_i) = 0.0032 + \frac{0.221}{Re_i^{0.237}}$

$$R_i = -\frac{f_i L}{4D_h\zeta}\left(\frac{F_c n}{F}\right)^2 = -0.0032\frac{L/D_h}{4\zeta}\left(\frac{F_c n}{F}\right)^2 - \frac{0.221(L/D_h)}{4(W_0 D_h/\nu)^{0.237}\zeta(W_i/W_0)^{0.237}}\left(\frac{F_c n}{F}\right)^2 = -\frac{0.0008E}{\zeta}M^2 - \frac{0.05525E}{Re_0^{0.237}\zeta}M^2 \quad (32)$$

Pressure recovery factors [2]

$$k_i = \alpha + 2\gamma\ln\frac{W_i}{W_0} = \alpha + 2\gamma\ln w_i \quad (33)$$

where α is the pressure recovery factor of the first port branch, and γ is the increment of the pressure recovery factor along the manifold. α-γ is the pressure recovery factor of the last port branch. The α and γ are dependent on the geometry of the manifold and independent on the velocity. Both α and γ should be determined through experiments.

Inserting Eq. (34) into Eq. (17), one obtains Q_i for the ith section,

$$Q_i = \frac{2-\beta_i}{3\zeta_i}\left(\frac{F_c n}{F}\right)^2 = \frac{2k_i}{3\zeta_i}\left(\frac{F_c n}{F}\right)^2 = \frac{2}{3\zeta_i}(\alpha + 2\gamma\ln w_i)\left(\frac{F_c n}{F}\right)^2 \quad (34)$$

5.2. Discrete solutions

The corresponding discrete solutions still depends on the sign of $Q^3 + R^2$. Herein we solve case for $R^2 + Q^3 > 0$. Interested readers can refer to Appendix C for further details of the cases ($R^2 + Q^3 < 0$ and $R^2 + Q^3 = 0$).

Axial velocity in the manifold

$$w_{i+1} = e^{-B_i x_{i+1}/2}\left[\frac{\sin(\sqrt{3}J_i(1-x_{i+1})/2)}{\sin(\sqrt{3}J_i/2)}\right] \quad (35)$$

$$w_0 = 1$$
$$w_n = 0$$

Port velocity

$$u_{c_{i+1}} = \left(\frac{F}{2nF_c}\right)e^{-B_i x_{i+1}/2}\left[\frac{B_i\sin(\sqrt{3}J_i(1-x_{i+1})/2) + \sqrt{3}J_i\cos(\sqrt{3}J_i(1-x_{i+1})/2)}{\sin(\sqrt{3}J_i/2)}\right] \quad (36)$$

Flow distribution

$$v_{c_{i+1}} = \frac{1}{2}e^{-B_i x_{i+1}/2}\left[\frac{B_i\sin(\sqrt{3}J_i(1-x_{i+1})/2) + \sqrt{3}J_i\cos(\sqrt{3}J_i(1-x_{i+1})/2)}{\sin(\sqrt{3}J_i/2)}\right] \quad (37)$$

Pressure drop in the ports

$$p_{i+1} - p_{c_{i+1}} = \left(\frac{\zeta}{2}\right)\left(\frac{F}{nF_c}\right)^2 e^{-B_i x_{i+1}}\left[\frac{B_i\sin(\sqrt{3}J_i(1-x_{i+1})/2) + \sqrt{3}J_i\cos(\sqrt{3}J_i(1-x_{i+1})/2)}{2\sin(\sqrt{3}J_i/2)}\right]^2 \quad (38)$$

Pressure drop in the manifold

$$p_{i+1} - p_0 = \frac{Lf_i}{4D_h B_i\sin^2(\sqrt{3}J_i/2)}(e^{-B_i x_{i+1}} - 1) - \frac{Lf_i}{4D_h(B_i^2 + 3J_i^2)\sin^2(\sqrt{3}J_i/2)}$$
$$\{B_i e^{-B_i x_{i+1}}\cos[\sqrt{3}J_i(1-x_{i+1})] - \sqrt{3}J_i e^{-B_i x_{i+1}}\sin[\sqrt{3}J_i(1-x_{i+1})] +$$
$$B_i\cos(\sqrt{3}J_i) + \sqrt{3}J_i\sin(\sqrt{3}J_i)\} - k_i\frac{e^{-B_i x_{i+1}}\sin^2[\sqrt{3}J_i(1-x_{i+1})/2]}{\sin^2(\sqrt{3}J_i/2)} \quad (39)$$

Unlike a conventional discrete approach, a successive approximation or iteration is not required while the present explicit solutions are used for varying factors and discrete manifolds. For example, Eq. (23) is substituted by a difference equation (Eq. (35)) for the $(i+1)$th section. The inlet velocity, w_0, can be used for calculation of the friction and the pressure recovery factors at the entrance using Eqs. (28) and (33). Then, they are used for calculations of the parameters r_{1_0} and r_{2_0}. Thus, we can calculate the next velocity, w_1, using the discrete equation (35). The w_1 can be used step-forward for calculation of the friction and the pressure recovery factors in the next section and the velocity, w_2. The procedure ends up to $i = n$. A similar procedure can be employed for calculation of the flow distribution (Eq. (37)) and the pressure drop (Eq. (38)).

Sample procedure of the step-forward calculations is as follows,

(1) calculate local Q_i and R_i,
(2) calculate r_{1_i} and r_{2_i},
(3) calculate the velocity in the $(i+1)$th section using Eq. (35) up to $i = n$,
(4) and similarly calculate flow distribution (Eq. (37)) and pressure drop (Eq. (38)) in the $(i+1)$th section up to $i = n$.

6. Results and discussions

It is clear that both the friction and the inertial term of the ordinary second order non-linear differential equation (Eq. (19)) are kept in the present solutions. This gives a three complete analytical solutions for the manifold, $R^2 + Q^3 < 0$, $R^2 + Q^3 = 0$ and $R^2 + Q^3 > 0$. It can be seen that there are clear terms of the friction and the momentum effects in Eq. (27) and Eq. (39). For example, the first two terms in the left hand of Eq. (27) represents the friction contribution, and the third term does the momentum contribution. These solutions can quantitatively describe interaction between the friction and the momentum. This confirms our previous results of the friction and the momentum interaction in Refs. [2,8].

Furthermore, a clear advantage in the present methodology over conventional discrete ones is that the procedure of design calculation is straightforward in reality without requirements of iteration, successive approximation and computer programme. There are three general characteristic parameters (E, M and ζ) to control flow distribution and pressure drop in manifolds. Here we demonstrate how to adjust systematically the three characteristic parameters in designs of manifolds. For the sake of convenience, we separate the manifold into ten sections for substitutions of varying friction and pressure recovery factors. Unless mentioned, $\alpha = 0.6$ and $\gamma = -0.15$ in the calculations of the pressure recovery factor, k (Eq. (33)). It should be mentioned that α and γ are only dependent on manifold geometry. They should be calibrated for a specific geometry if data is not available.

6.1. A comparison of velocity profile between constant and varying factors

Fig. 4 shows a comparison of velocity profile between the varying and the constant factors. It can be seen that the curve ($k = 0.6$) is most closed to that of the varying factors. This is because the present α is equal to 0.6. We know that the α in Eq. (33) represents the pressure recovery factor of the first port/section in the cases of the varying factors. That means the same effect of the momentum on the first section if $k = \alpha$. When $k \neq \alpha$, it can be found that there is a big difference between the constant and the varying factors. Furthermore, the effect the friction is also the same since the velocity at the entrance is the same for both the constant and the varying factors. Thus, the curves with the constant factor overlap that with the varying factors at the first section. It is also found that the effect

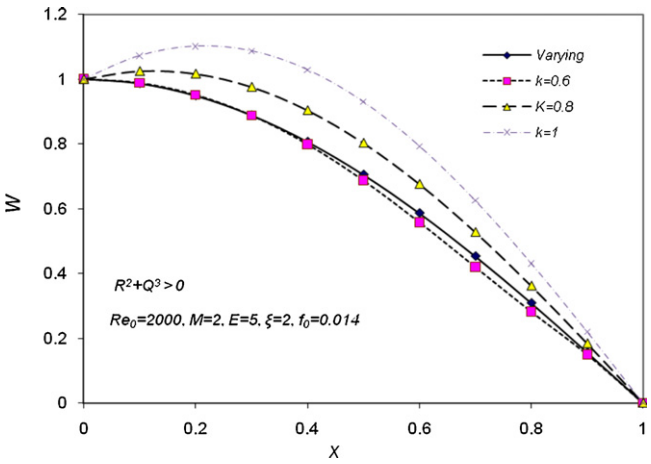

Fig. 4. A comparison of velocity profile between constant and varying pressure recovery factors.

of the momentum increases gradually along axial direction because the momentum factor increases. Nevertheless, there is a slight difference between the constant and the varying factors even at the best k (= 0.6).

Fig. 5 shows the effect of the constant friction factors on flow distribution in the ports. A flow distribution under variation of the friction and the pressure recovery factors is also given for a comparison. It can be seen that there is a difference between constant and varying factors at the end of the manifold. The effect of f on flow distribution in the ports is similar as those with the varying factors in the former half manifold because the inlet velocity is the same for all the friction factors. However, there is a difference between the constant and the varying factors at the end of the manifold because the constant friction factor is the same as that at the entrance and the varying one has been corrected. Finally, there is a little influence of constant factor change on flow distribution in the ports. It is because the flow is in the region controlled by the momentum so that influence of f on flow distribution in the ports was suppressed. It should be noted that there is almost the same values between constant and varying factors when $x = 0.5$. This is in agreement with the results of Ref. [2]. The calculated friction loss using the constant factors is less than those using varying factors at the former half manifold; the loss is greater at the latter half. This

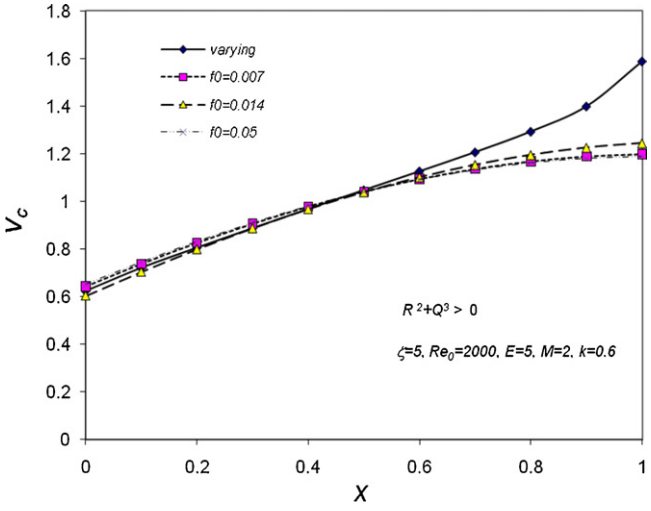

Fig. 5. A comparison of flow distribution between constant and varying friction factors.

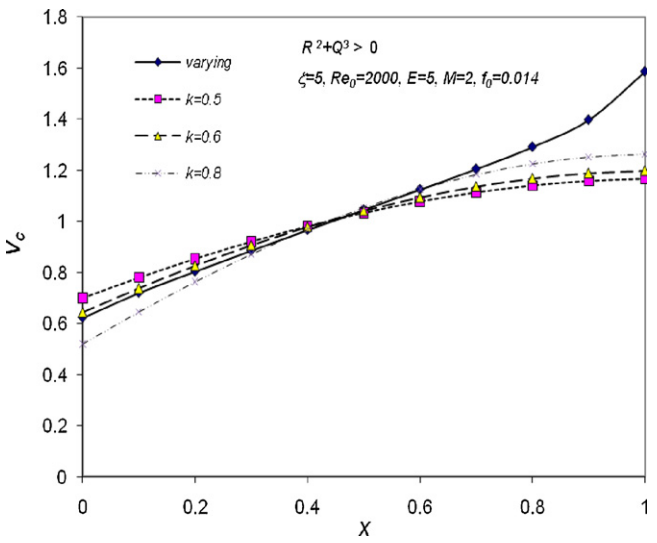

Fig. 6. A comparison of flow distribution between constant and varying pressure recovery factors.

can be explained that a less f can be expected at the former half because the velocity in the former half is greater than those in the latter one.

Fig. 6 shows a comparison of the flow distribution between the constant and the varying pressure recovery factors. It can be found that there is a significant influence of the constant k on the flow distribution. This means that the flow branching affects significantly flow distribution. It should be noted that the former half of the curve with $k = 0.6$ nearly overlaps those of the varying factors. This is in agreement with those in Fig. 4. When $k = \alpha$, the effect of the momentum is the same in the first section. When $k \neq \alpha$, the flow distribution with the constant factors will deviate from that with the varying factors. At $x = 0.5$ there is almost same values between the constant and the varying factors former half manifold. At two ends the effect increases along x-axis due to increase of k change. This is in agreement with the results of Ref. [2] in which an ideal analytical solution was obtained under assumption of linear velocity profile. According to the analysis in Ref. [2], there is a corrective term in the varying solution, which varies with x and explains momentum effect due to varying velocity along the manifold. The present results show that there is a significant difference of flow distribution between the constant and the varying factors in the latter half manifold. A proper selection of k does improve the solution of the constant factors. This provides direct evidences how the factors affect the flow distribution.

6.2. Effect of ratio of length to diameter on flow distribution

Fig. 7 shows influence of the structure parameter E on axial velocity, flow distribution and pressure drop along the manifold. The linear axial velocity can be approached only when E is smaller as shown in Fig. 7a. An increase in E can result in non-linear. This is because a certain momentum always needs a corresponding friction balance. A larger E means an increase of friction resistance along the manifold. Thus, it needs more momentum to balance the friction effect. However, a proper selection of E does improve uniformity after other parameters are fixed. Therefore, it is possible to have a design with linear axial velocity when a set of proper structure parameters are selected.

The influence of the structure parameter E on the flow distribution and the pressure drop in the ports is shown in Fig. 7b and c, respectively. The uniform distribution can be found only when E is smaller again. Any increase of E will result in non-uniformity.

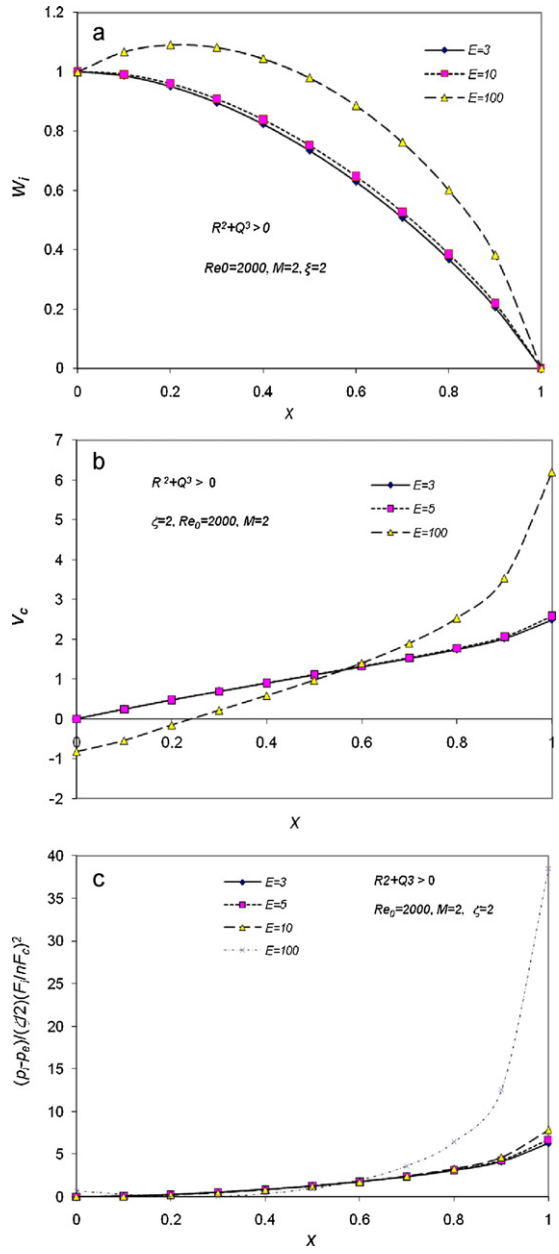

Fig. 7. Effects of ratio of manifold length to diameter, E, on velocity profile, flow distribution and pressure drop: (a) velocity profile, (b) flow distribution, (c) pressure drop.

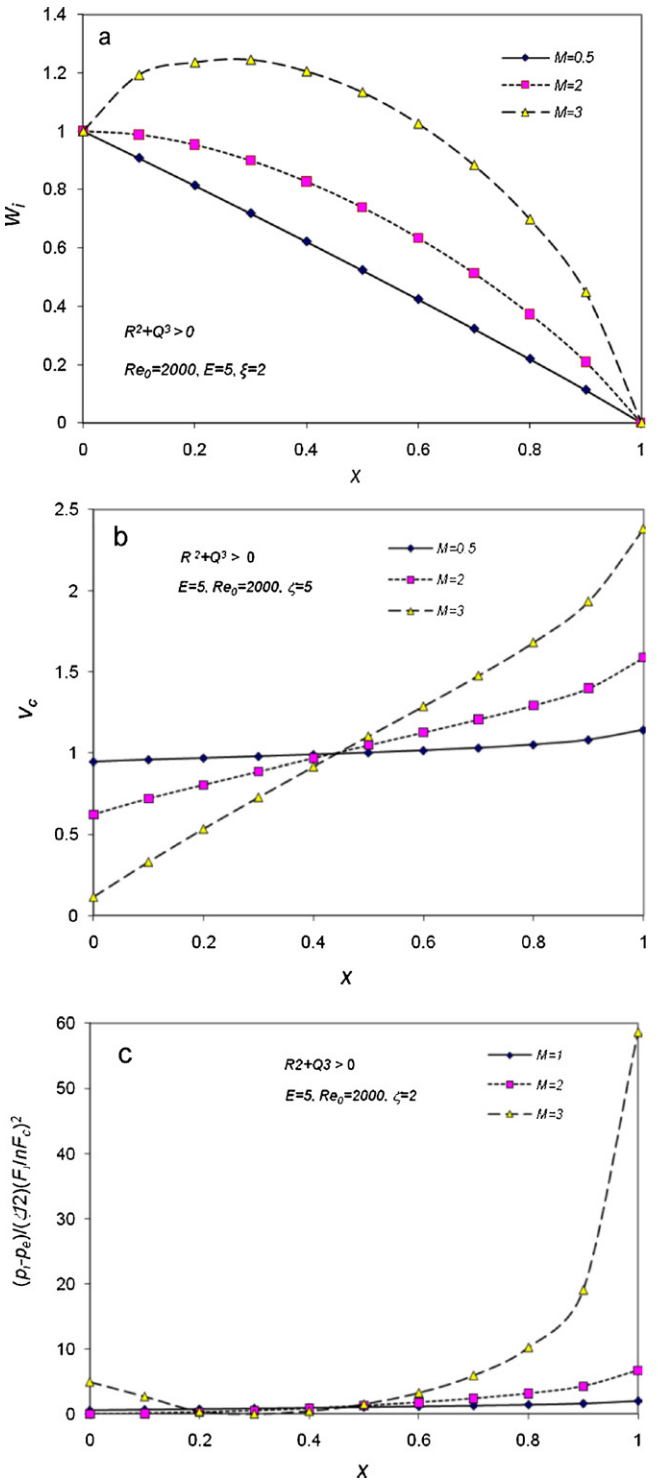

Fig. 8. Effects of M (ratio of sum of all the port areas to the area of the manifold, $F_c n/F$) on velocity profile, flow distribution and pressure drop: (a) velocity profile, (b) flow distribution, (c) pressure drop.

This is in agreement with those of Fig. 7a. However, it can be found that there is a similar flow distribution when $E < 5$. This means that the influence of E can be neglected when E is lower than a value. Furthermore, it is difficult to have a uniform flow distribution and pressure drop if only parameter E is adjusted. A set of proper structure parameters has to be adjusted to achieve an appreciated flow distribution.

6.3. *Effect of M (ratio of sum of all the ports areas to area of the manifold, $F_c n/F$) on flow distribution and pressure drop*

Fig. 8 shows influence of the structure parameter M on axial velocity, flow distribution and pressure drop along the manifold. There is a significant influence of M on the axial velocity profile. The axial velocity can be approached when M is smaller. At the extreme condition (i.e., $M = 0$), there is no the effect of the flow branching. Thus, an absolute uniform flow distribution can be expected. The uniform distribution can be found only when M is smaller. This is because a certain momentum always needs a corresponding friction balance. For a larger M, the momentum cannot balance the friction effect, resulting in a non-uniform flow distribution. Any increase of M will result in non-uniformity. However, a proper selection of M does improve uniformity of pressure drop. This is in agreement in those in Ref. [2]. Therefore, it is possible to have

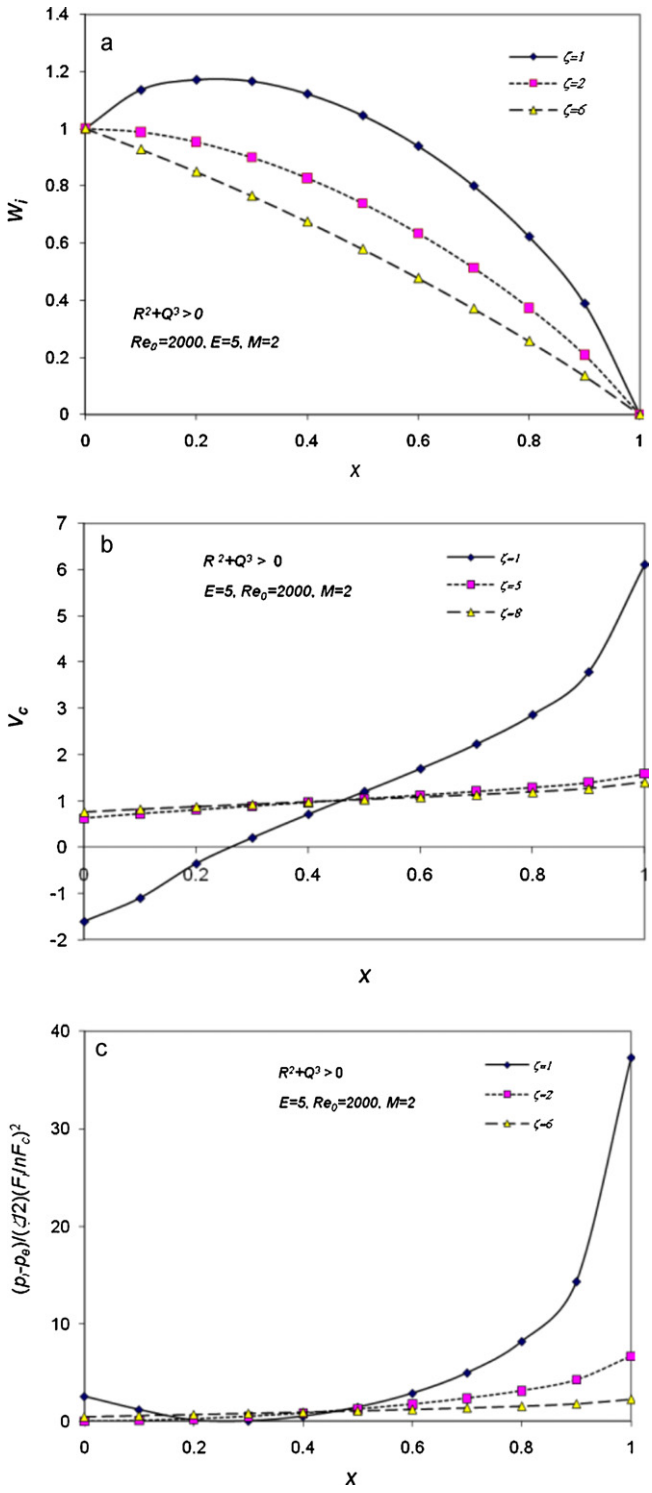

Fig. 9. Effects of total head loss coefficients of ports on velocity profile, flow distribution and pressure drop: (a) velocity profile, (b) flow distribution, (c) pressure drop.

a uniform pressure drop design when a set of proper structure parameters is selected.

6.4. Effect of total head loss coefficients of ports on velocity profile, flow distribution and pressure drop

Fig. 9 shows influence of the structure parameter ζ on axial velocity, flow distribution and pressure drop along the manifold. The structure parameter ζ represents the resistance of outflow through ports. It can be seen that there is a significant influence of ζ on the axial velocity profile, flow distribution and pressure drop. The uniform flow distribution can be approached as increases. At an extreme condition when $\zeta \to \infty$, the manifold will be a closed system and an absolute uniform distribution can be found. However, a proper selection of ζ does improve uniformity of pressure drop. This is because a big ζ means bigger resistance in ports. The flow will prefer to enter lower resistant paths in the manifold. Thus, the flow will be distributed more uniformly in the manifold. This offers a possibility to adjust ζ for improvement of flow distribution and pressure drop.

6.5. Effect of inlet Reynolds number on flow distribution and pressure drop

Fig. 10 shows influence of the inlet Reynolds number on flow distribution and pressure drop along the manifold. It can be seen that there is a little influence of the inlet Reynolds number on the flow distribution and pressure drop when E is smaller (see Fig. 10a and b). This is because the effect of the momentum is dominated in a small E manifold so that the effect of the friction can be neglected. This is also in agreement with the previous empirical results that the friction term can be neglected for a short manifold [22]. However, it can be found that there is a significant influence when E is larger (see Fig. 10c). This demonstrates significance of interaction between flow performance and manifold structure. For a larger E manifold, the effect of the friction can become dominant because the effect of the velocity on the friction factor increases. Thus, the inlet Reynolds number becomes important on flow distribution. This shows complexity of fluid and structure interaction. An isolated consideration may result in the failure of uniform design.

6.6. A comparison of flow distribution between two sets of Reynolds numbers and M

Fig. 11 shows a comparison of flow distributions between two sets of Reynolds numbers and M. It can be found that the M does affect significantly flow distribution in the same inlet Reynolds number. For the same inlet Reynolds number the uniformity increases as M decreases at a fixed E (=5) and ζ (=5). The inlet Reynolds number has a little influence in this structure and flow conditions. However, although there is a slight difference at the end of the manifold it can be neglected due to Reynolds number change. For the small difference at the end of the manifold it can be explained that a larger Reynolds number represents smaller friction and larger pressure recovery coefficients in the momentum equation, resulting in a large momentum effect.

A comparison of pressure drop between two sets of inlet Reynolds numbers and M is shown in Fig. 12. It can be seen that the pressure drop is greatly dependent on ratio of sum of all the port areas to manifold cross-sectional area. Again there is a small influence of the inlet Reynolds number on pressure drop in this flow region and manifold structure at a fixed E (=5) and ζ (=2). A small influence of inlet Reynolds number means that change of operational conditions may be inadequate results for any uniform design of flow distribution and pressure drops.

6.7. Application of the present analytical solution to designs of manifolds

Fig. 13 shows influence of the structure parameters pitch on flow distributions when Re_0 = 2000, E = 5, M = 2 and ζ = 5. It can be seen that the effect of n on the flow distribution is obvious. However, there exists a threshold n_c. When $n > n_c$ the effect of n can be neglected. It is interesting that there is a significant influence at the

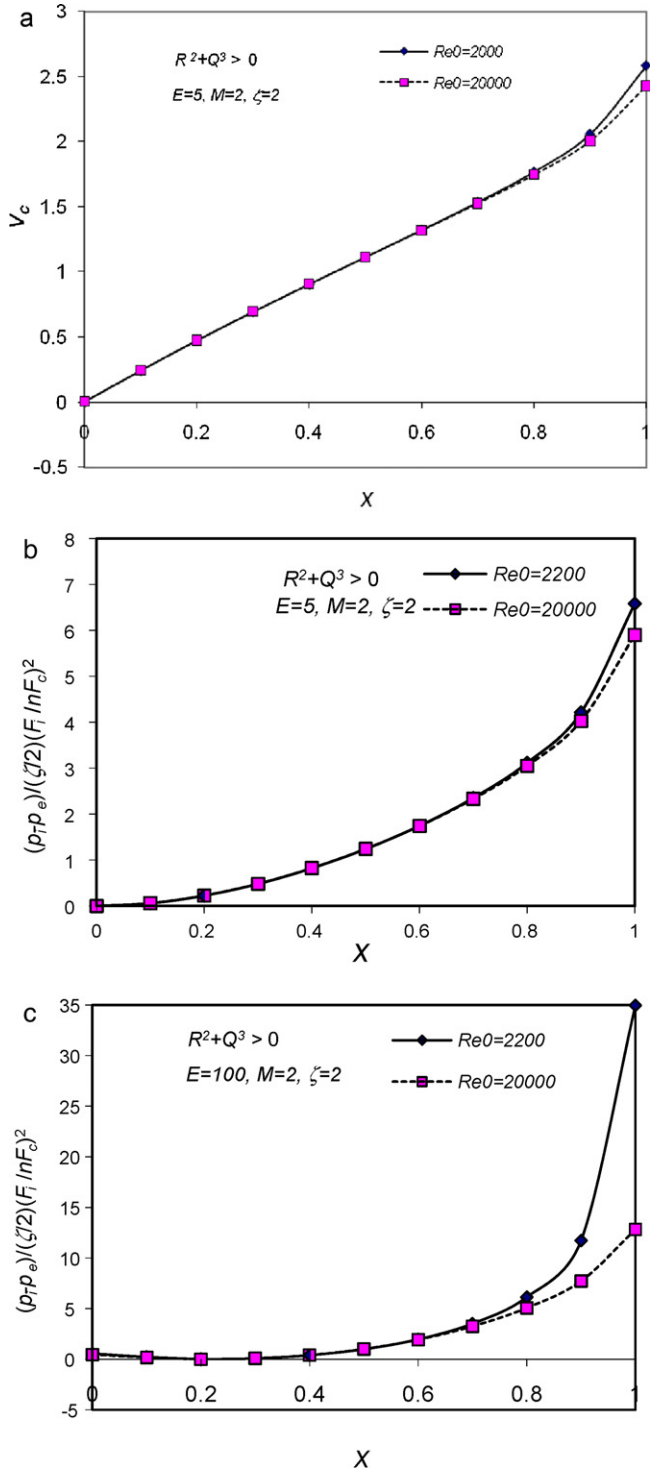

Fig. 10. Effect of inlet Reynolds number on flow distribution and pressure drop: (a) flow distribution, (b) pressure drop for a small E and (c) pressure drop for a big E.

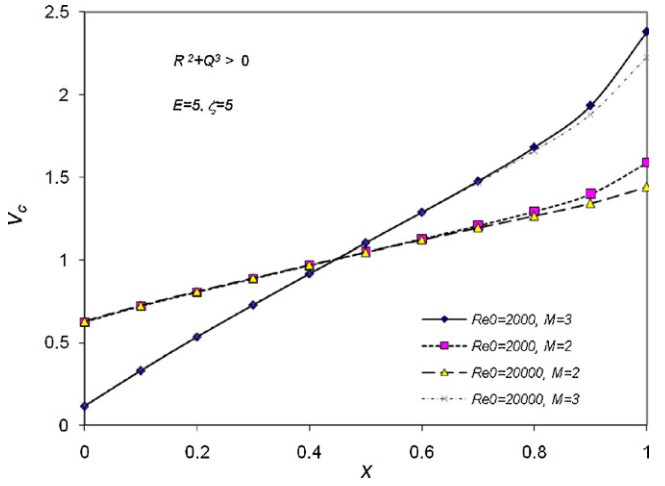

Fig. 11. A comparison of flow distribution between two Reynolds numbers when $E = 5$.

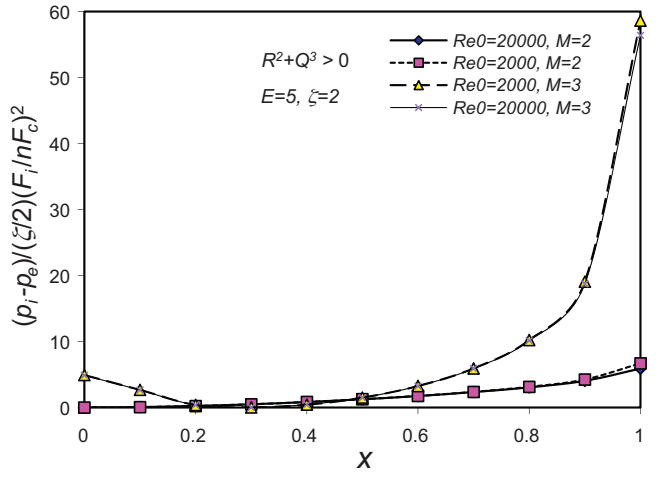

Fig. 12. A comparison of pressure drop between two Reynolds numbers when $E = 100$.

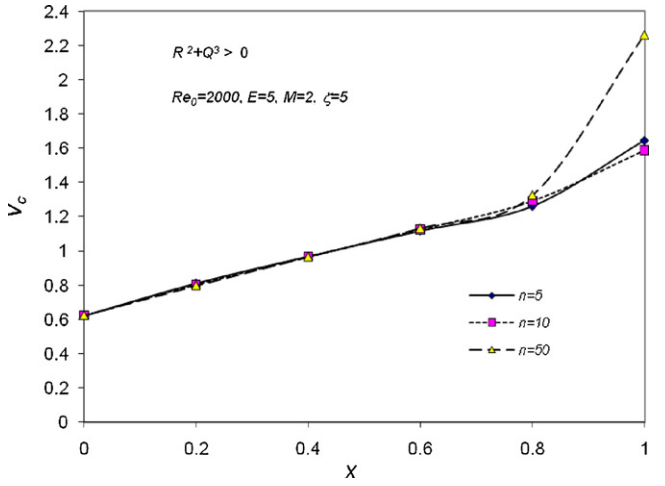

Fig. 13. Effect of varying number of sections or ports on flow distribution.

end of the manifold. This may be explained that an increase of port number is related to corresponding increase of momentum effect. This case shows that the uniform design of the flow distribution can be adjusted by a pitch change. It also shows that it is possible to use the present analytical solutions for the design of the discrete manifolds.

The parameter ζ can be adjusted locally by using throttle rings or adjustment of port length. Thus this provides further measures to adjust flow distribution in the ports along the manifold. The effect of ζ on the flow distribution is shown in Fig. 14. When a same ζ (= 2) is used for the former six sections/ports, we adjust the ζ in the latter half manifold to be equal to 5, 6, 7, 8, and 9, respectively. A varying ζ along the manifold does improve the flow distribution for the latter five ports. This is because a higher ζ means a bigger fric-

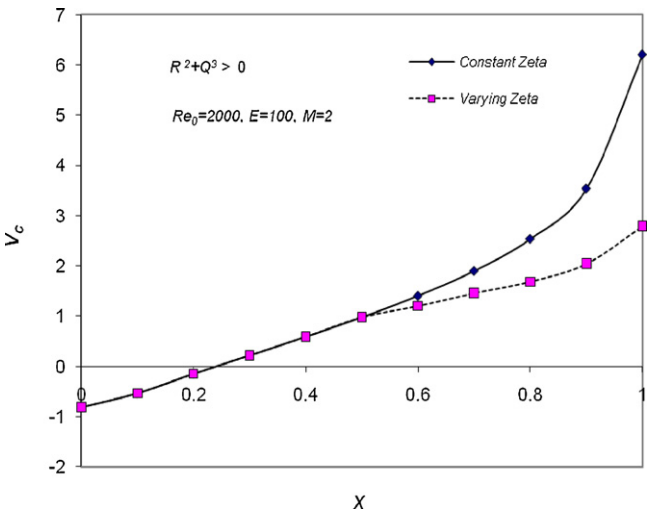

Fig. 14. Effect of varying ζ along manifold on flow distribution.

tion, and restrain flow through these ports. Therefore, the flow will prefer to enter lower resistant paths. It is possible to have a uniform flow distribution when a proper adjustment of resistance in ports is performed. The theory does give a guideline how to adjust manifold structures and flow condition to improve flow distribution.

All the results demonstrate the capacity of the present models for preliminary design optimisation. Measurable progress has been achieved in the development of mathematical models and the solution methodology in the past fifty years, particularly in the recent fifteen years. The present model has overcome all the three limitations of Acrivos et al.'s. The present model provides valuable tools for the elucidation of the underlying mechanisms and prediction of the distribution process under consideration Acrivos et al.'s model is not the most generalised in this field. In practice, Kulkarni et al. [18] carried out a comparison among three theoretical models. Their results showed that the model of Acrivos et al. overpredicted pressure at the dead end, as shown in Fig. 8 of Ref. [18] and the model of Wang et al. was in agreement with experimental data. Although the statement of Kulkarni et al. [18,32] is misleading it is useful in provoking a deeper examination of flow modelling in manifold systems.

These completed analytical solutions have two separated terms to quantitatively describe effects of the friction and momentum in a manifold. The results showed explicitly opposite influence between the friction and the momentum. This proves theoretically interaction between the friction and the momentum again which is in agreement with our previous results in Refs. [2,8]. It is obvious that the conventional manifold may experience severe problems of non-uniform flow distribution. Some ports are starved of fluids, while others may have them in excess. Since friction and momentum effects work in opposite directions, a proper adjustment does improve flow distribution. The present results show that there are three general characteristic parameters (E, M and ζ) to control flow distribution and pressure drop in manifolds. However, adjustments of these parameters are not straightforward due to complexity of flow in manifolds. There is a significant difference of the friction factor and the pressure recovery factors on flow distribution. At the former half manifold, the influence of the friction factor can be neglected and the pressure recovery factor will be determined by the first section value. At the latter half manifold, the influence of the friction factor can be important and the influence of the pressure recovery factor increases as well. An isolated consideration may result in the failure of uniform design. For example, when the momentum is dominated the adjustment of the parameters related to the friction may be suppressed. Therefore, the generalised model provides easy-to-use design guidance to investigate the interactions among structures, operating conditions and manufacturing tolerance through a systematic consideration under a wide variety of combination of flow conditions and geometries. The flow distribution can be improved greatly by integrated adjustment of all the parameters.

7. Conclusions

We examine development of theoretical models and methodologies of solutions in flow in manifolds and highlight remarkable advances in the past fifty years. The theoretical model of Acrivos et al. [31] was unified into the generalised model developed by Wang [27,28]. The main existing models have converged into one theoretical framework which is fundamentals of various models to study flow in manifolds.

The theoretical model is a powerful tool for the elucidation of the underlying mechanisms and prediction of flow distribution under consideration in which the flow distribution and pressure drop can be investigated under various flow conditions and geometrical parameters. The analytical solutions have two separated terms to quantitatively describe effects of the friction and the momentum in the manifold. The results prove theoretically interaction between the friction and the momentum again. The friction and the momentum effects work in opposite directions, the former tending to produce a pressure drop and the latter a pressure rise. Unlike conventional models, the present model is applicable to those cases in variation of the friction and the pressure recovery factors by using section by section replacement. The sensitivity of the friction and the pressure recovery factors was analysed to determine the influence of their variations. The influence of the friction factor and the pressure recovery factors on flow distribution at the former half manifold is different from that at the latter half manifold. This is in agreement with our previous results in Refs. [2,8].

The theoretical model is applicable not only to designs of continuum manifolds but also those of discrete ones for arbitrary shape of manifolds if using hydraulic diameter and wetted perimeter. For a discrete manifold, a clear advantage in the present methodology over conventional discrete ones is that the procedure of design calculation is straightforward in reality without requirements of iteration, successive approximation and computer programme. There are three general characteristic parameters (E, M and ζ) to control flow distribution and pressure drop in manifolds. The theory demonstrated how to adjust systematically the three characteristic parameters in designs of manifolds and to minimize the impact on manifold operability. Therefore, the generalised model provides easy-to-use design guidance to investigate the interactions among structures, operating conditions and manufacturing tolerance under a wide variety of combination of flow conditions and geometries.

Finally, in spite of complexity and difficulty, the rational yet tractable generalised model of this type can contribute to the shared goal of cutting the currently cost and performance improvement of new design and development of distributors, which is central to a chemical engineer's "toolbox". Measurable progress has been achieved in the development of mathematical models and the solution methodologies of flow in manifold systems in the past fifty years. The generalised theory makes a step forward in understanding of flow in manifold systems and offers a powerful tool for designs of manifold systems.

Acknowledgements

Rothamsted Research is supported by Biotechnology and Biological Sciences Research Council (BBSRC). The author thanks the

editor and two anonymous reviewers for their comments and suggestions to improve the manuscript.

Appendix A.

Analytical solution of differential equations of flow in manifolds.

Eq. (20) is a second order nonlinear ordinary differential equation. To solve Eq. (20), we assume that the function, $w_i = e^{rx}$, is a solution of Eq. (20) and substitute it and its derivatives into Eq. (20), we obtain the characteristic equation of Eq. (20).

$$r^3 + 3Qr - 2R = 0 \tag{A1}$$

To solve cubic equation Eq. (A1), let B and A be arbitrary constants, and an identity satisfied by perfect cubic polynomial is

$$r^3 - B^3 = (r - B)(r^2 + Br + B^2) \tag{A2}$$

Adding $A(r-B)$ to both sides of Eq. (A2)

$$r^3 - B^3 + A(r - B) = (r - B)(r^2 + Br + B^2 + A) = 0 \tag{A3}$$

Which after regrouping terms, is:

$$r^3 + Ar - (B^3 + BA) = (r - B)[r^2 + Br + (B^2 + A)] = 0 \tag{A4}$$

We would like to match the coefficients A and $-(B^3 + BA)$ in Eq. (A4) with those of Eq. (A1), and we have

$$A = 3Q \quad B^3 + BA = 2R \tag{A5}$$

Inserting the former into the latter then gives,

$$B^3 + 3QB = 2R \tag{A6}$$

The trial solution accomplishing this miracle turns out to be the symmetrical expression

$$B = [R + \sqrt{Q^3 + R^2}]^{1/3} + [R - \sqrt{Q^3 + R^2}]^{1/3} \tag{A7}$$

Therefore, we have found a value of B satisfying the above identity of Eq. (A4), and we have factored a linear term $(r-B)$ from the cubic of Eq. (A1), thus reducing it to a quadratic equation. We need now only factor the quadratic part. Inserting $A = 3Q$ into the quadratic part of Eq. (A3) and solving the resulting

$$r^2 + Br + (B^2 + 3Q) = 0 \tag{A8}$$

Then gives the solutions

$$\begin{aligned} r &= \frac{1}{2}[-B \pm \sqrt{B^2 - 4(B^2 + 3Q)}] \\ &= \frac{1}{2}(-B \pm \sqrt{-3B^2 - 12Q}) \\ &= -\frac{1}{2}B \pm \frac{1}{2}\sqrt{3}i\sqrt{B^2 + 4Q} \end{aligned} \tag{A9}$$

Therefore, at last, the roots of the original equation in r are then given by

$$\begin{cases} r = [R + \sqrt{Q^3 + R^2}]^{1/3} + [R - \sqrt{Q^3 + R^2}]^{1/3} \\ r_1 = -\frac{1}{2}B + \frac{1}{2}\sqrt{-3(B^2 + 4Q)} \\ r_2 = -\frac{1}{2}B - \frac{1}{2}\sqrt{-3(B^2 + 4Q)} \end{cases} \tag{A10}$$

These can be simplified by defining

$$J = [R + \sqrt{Q^3 + R^2}]^{1/3} - [R - \sqrt{Q^3 + R^2}]^{1/3} \tag{A11}$$

$$\begin{aligned} J^2 &= [R + \sqrt{Q^3 + R^2}]^{2/3} - 2[R^2 - (Q^3 + R^2)]^{1/3} + [R - \sqrt{Q^3 + R^2}]^{2/3} \\ &= [R + \sqrt{Q^3 + R^2}]^{2/3} + [R - \sqrt{Q^3 + R^2}]^{2/3} + 2Q \\ &= B^2 + 4Q \end{aligned} \tag{A12}$$

That is

$$\begin{cases} r = B \\ r_1 = -\frac{1}{2}B + \frac{1}{2}i\sqrt{3}J \\ r_2 = -\frac{1}{2}B - \frac{1}{2}i\sqrt{3}J \end{cases} \tag{A13}$$

Appendix B.

The solutions of Eq. (19) depends on the sign of $Q^3 + R^2$, which have three cases. The solutions of two cases ($Q^3 + R^2 < 0$ and $Q^3 + R^2 = 0$) are listed here.Case 1: $R^2 + Q^3 < 0$

For $Q^3 + R^2 < 0$, defining $\theta = \cos^{-1}(R/\sqrt{-Q^3})$, and substituting it into Eqs. (A13) and (A13) can be reduced to:

$$r_1 = 2\sqrt{-Q}\cos\left(\frac{\theta}{3}\right)$$

$$r_2 = 2\sqrt{-Q}\cos\left(\frac{\theta + 2\pi}{3}\right)$$

Thus, the general solution of Eq. (19) and boundary conditions can be written as follows:

$$\begin{aligned} &w = C_1 e^{r_1 x} + C_2 e^{r_2 x} \\ &w = 0, \quad at \quad x = 1 \\ &w = 1, \quad at \quad x = 0 \end{aligned} \tag{B1}$$

Axial velocity in the manifold:

$$w = \frac{e^{r_1 + r_2 x} - e^{r_2 + r_1 x}}{e^{r_1} - e^{r_2}} \tag{B2}$$

Port velocity by substituting Eq. (B1) into Eq. (8):

$$u_c = -\frac{F_i}{nF_c}\frac{r_2 e^{r_1 + r_2 x} - r_1 e^{r_2 + r_1 x}}{e^{r_1} - e^{r_2}} \tag{B3}$$

Flow distribution through Eq. (B3):

$$v_c = \frac{F_c U_c}{F_i W_0/n} = \left(\frac{nF_c}{F_i}\right) u_c = -\frac{r_2 e^{r_1 + r_2 x} - r_1 e^{r_2 + r_1 x}}{e^{r_1} - e^{r_2}} \tag{B4}$$

Pressure drop in the ports after substituting Eq. (B2) into Eq. (15):

$$p - p_c = \frac{\zeta}{2}\left(\frac{F}{nF_c}\right)^2 \left(\frac{r_2 e^{r_1 + r_2 x} - r_1 e^{r_2 + r_1 x}}{e^{r_1} - e^{r_2}}\right)^2 \tag{B5}$$

Pressure drop in the manifold after substituting Eq. (B2) into Eq. (14) and integrating Eq. (14):

$$\begin{aligned} p - p_0 = -\frac{Lf}{2D_h(e^{r_1} - e^{r_2})^2}\{&\frac{1}{2r_2}e^{2(r_1 + r_2 x)} - \frac{2}{r_1 + r_2}e^{(r_1 + r_2)(1 + x)} + \frac{1}{2r_1}e^{2(r_2 + r_1 x)} - \\ &\frac{1}{2r_2}e^{2r_1} + \frac{2}{r_1 + r_2}e^{(r_1 + r_2)} - \frac{1}{2r_1}e^{2r_2}\} - \frac{2 - \beta}{2}\frac{(e^{r_1 + r_2 x} - e^{r_2 + r_1 x})^2}{(e^{r_1} - e^{r_2})^2} \end{aligned} \tag{B6}$$

For $R^2 + Q^3 = 0$, Two conjugated solutions of the characteristic equation can be reduced as follows:

$$r_1 = r_2 = -\frac{1}{2}R^{1/3} = r$$

Thus, the general solution of Eq. (19) and its boundary conditions can be written as follows:

$$\begin{aligned} &w = (C_1 + C_2 x)e^{rx} \\ &w = 0, \quad at \quad x = 1 \\ &w = 1, \quad at \quad x = 0 \end{aligned} \tag{B7}$$

Axial velocity in the manifold:

$$w = (1 - x)e^{rx} \tag{B8}$$

Port velocity by substituting Eq. (B8) into Eq. (8):

$$u_c = -\frac{F}{nF_c}(r - 1 - rx)e^{rx} \tag{B9}$$

Flow distribution using Eq. (B9)

$$v_c = \left(\frac{nF_c}{F}\right) u_c = -(r - 1 - rx)e^{rx} \tag{B10}$$

Pressure drop in the ports after substituting Eq. (B8) into Eq. (15):

$$p - p_c = \frac{\zeta}{2}\left(\frac{F}{nF_c}\right)^2 (r - 1 - rx)^2 e^{2rx} \tag{B11}$$

Pressure drop in the manifold after substituting Eq. (B8) into Eq. (14) and integrating Eq. (14):

$$\begin{aligned} p - p_0 = &-\frac{Lf}{4D_h r}\{e^{2rx}(1-x)^2 + 2e^{2rx}(1-x) + \frac{1}{r}e^{2rx} - 3 - \frac{1}{r}\} \\ &-\frac{2-\beta}{2}(1-x)^2 e^{2rx} \end{aligned} \tag{B12}$$

Appendix C.

After substituting R_i and Q_i into analytical solutions, the corresponding discrete solutions of two cases ($Q^3 + R^2 < 0$ and $Q^3 + R^2 = 0$) are listed for the $(i+1)$th section.

For $R^2 + Q^3 < 0$, Axial velocity in the manifold

$$w_{i+1} = \frac{e^{r_{1_i}+r_{2_i}x_{i+1}} - e^{r_{2_i}+r_{1_i}x_{i+1}}}{e^{r_{1_i}} - e^{r_{2_i}}} \qquad i = 1, \cdots, n \tag{C1}$$

$$w_0 = 1$$
$$w_n = 0$$

where n is the number of ports/sections.Port velocity

$$u_{c_{i+1}} = \frac{F}{nF_c}\frac{r_{2_i}e^{r_{1_i}+r_{2_i}x_{i+1}} - r_{1_i}e^{r_{2_i}+r_{1_i}x_{i+1}}}{e^{r_{1_i}} - e^{r_{2_i}}} \tag{C2}$$

Flow distribution

$$v_{c_{i+1}} = -\frac{r_{2_i}e^{r_{1_i}+r_{2_i}x_{i+1}} - r_{1_i}e^{r_{2_i}+r_{1_i}x_{i+1}}}{e^{r_{1_i}} - e^{r_{2_i}}} \tag{C3}$$

Pressure drop in the ports

$$p_{i+1} - p_{c_{i+1}} = \frac{\zeta}{2}\left(\frac{F}{nF_c}\right)^2 \left(\frac{r_{2_i}e^{r_{1_i}+r_{2_i}x_{i+1}} - r_{1_i}e^{r_{2_i}+r_{1_i}x_{i+1}}}{e^{r_{1_i}} - e^{r_{2_i}}}\right)^2 \tag{C4}$$

Pressure drop in the manifold

$$\begin{aligned} p_{i+1} - p_0 = &-\frac{Lf_i}{2D_h(e^{r_{1_i}} - e^{r_{2_i}})^2}\{\frac{1}{2r_{2_i}}e^{2(r_{1_i}+r_2x_{i+1})} \\ &-\frac{2}{r_{1_i}+r_{2_i}}e^{(r_{1_i}+r_{2_i})(1+x_{i+1})} + \frac{1}{2r_{1_i}}e^{2(r_{2_i}+r_{1_i}x_{i+1})} \\ &-\frac{1}{2r_{2_i}}e^{2r_{1_i}} + \frac{2}{r_{1_i}+r_{2_i}}e^{(r_{1_i}+r_{2_i})} - \frac{1}{2r_{1_i}}e^{2r_{2_i}}\} \\ &-k_i\frac{(e^{r_{1_i}+r_{2_i}x_{i+1}} - e^{r_{2_i}+r_{1_i}x_{i+1}})^2}{(e^{r_{1_i}} - e^{r_{2_i}})^2} \end{aligned} \tag{C5}$$

For $R^2 + Q^3 = 0$, Axial velocity in the manifold

$$w_{i+1} = (1 - x_{i+1})e^{r_i x_{i+1}} \tag{C6}$$

$$w_0 = 1$$
$$w_n = 0$$

Port velocity

$$u_{c_{i+1}} = -\frac{F}{nF_c}(r_i - 1 - r_i x_{i+1})e^{r_i x_{i+1}} \tag{C7}$$

Flow distribution

$$v_{c_{i+1}} = -(r_i - 1 - r_i x_{i+1})e^{r_i x_{i+1}} \tag{C8}$$

Pressure drop in the ports

$$p_{i+1} - p_{c_{i+1}} = \frac{\zeta}{2}\left(\frac{F}{nF_c}\right)^2 (r_i - 1 - r_i x_{i+1})^2 e^{2r_i x_{i+1}} \tag{C9}$$

Pressure drop in the manifold

$$\begin{aligned} p_{i+1} - p_0 = &-\frac{Lf_i}{4D_h r_i}\{e^{2r_i x_{i+1}}(1 - x_{i+1})^2 + 2e^{2r_i x_{i+1}}(1 - x_{i+1}) \\ &+\frac{1}{r_i}e^{2r_i x_{i+1}} - 3 - \frac{1}{r_i}\} \\ &-k_i(1 - x_{i+1})^2 e^{2r_i x_{i+1}} \end{aligned} \tag{C10}$$

References

[1] R.L. Pigford, M. Ashraf, Y.D. Mlron, Flow distribution in piping manifolds, Ind. Eng. Chem. Fundam. 22 (1983) 463–471.
[2] J.Y. Wang, Z.L. Gao, G.H. Gan, D.D. Wu, Analytical solution of flow coefficients for a uniformly distributed porous channel, Chem. Eng. J., 84 (1) 1–6.
[3] N.S. Hanspal, A.N. Waghode, V. Nassehi, R.J. Wakeman, Development of a predictive mathematical model for coupled stokes/Darcy flows in cross-flow membrane filtration, Chem. Eng. J. 149 (2009) 132–142.
[4] F. Kamisli, Laminar flow of a non-Newtonian fluid in channels with wall suction or injection, Int. J. Eng. Sci. 44 (2006) 650–661.
[5] F. Kamisli, Second law analysis of a disturbed flow in a thin slit with wall suction and injection, Int. J. Heat Mass transfer. 51 (2008) 3985–4001.
[6] R.A. Bajura, A model for flow distribution in manifolds, J. Eng. Power 98 (1971) 654–665.
[7] Z.Q. Miao, T.M. Xu, Single phase flow characteristics in the headers and connecting tube of parallel tube platen systems, Appl. Thermal Eng. 26 (2006) 396–402.
[8] J.Y. Wang, G.H. Priestman, D.D. Wu, A theoretical analysis of uniform flow distribution for the admission of high-energy fluids to steam surface condenser, J Eng. Gas Turbine Power 123 (2) (2001) 472–475.
[9] H.T. Chou, H.C. Lei, Outflow uniformity along a continous manifold, J. Hydraulic Eng. 134 (9) (2008) 1383–1388.
[10] A.A. Anwar, Friction crorrection factors for center-pivots, J Irrig. Drain. Eng. 125 (5) (1999) 280–286.
[11] A.A. Anwar, Adjusted factor Ga for pipelines with multiple outlets and outflow, J Irrig. Drain. Eng. 125 (6) (1999) 355–359.
[12] C. Amador, A. Gavriilidis, P. Angeli, Flow distribution in different microreactor scale-out geometries and the effect of manufacturing tolerances and channel blockage, Chem. Eng. J. 101 (2004) 379–390.
[13] H. Liu, P.W. Li, J.V. Lew, CFD study on flow distribution uniformity in fuel distributors having multiple structural bifurcations of flow channels, Int. J. Hydrogen Energy 35 (2010) 9186–9198.
[14] M. Heggemann, S. Hirschberg, L. Spiegel, C. Bachmann, CFD simulation and experimental validation of fluid flow in liquid distributors, Trans IChemE, Part A, Chem. Eng. Res. Design 85 (A1) (2007) 59–64.
[15] O. Tonomura, S. Tanaka, M. Noda, M. Kano, S. Hasebe, I. Hashimoto, CFD-based optimal design of manifold in plate-fin microdevices, Chem. Eng. J. 101 (2004) 397–402.
[16] A.W. Chen, E.M. Sparrow, Turbulence modelling for flow in a distribution manifold, Int. J. Heat Mass Transfer. 52 (2009) 1573–1581.
[17] J. Yuan, M. Rokni, B. Sunsen, Simulation of fully developed laminar heat and mass transfer in fuel cell ducts with different cross-sections, Int. J. Heat Mass Transfer. 44 (2001) 4047–4058.
[18] A.V. Kulkarni, S.S. Roy, J.B. Joshi, Pressure and flow distribution in pipe and ring spargers: Experimental measurements and CFD simulation, Chem. Eng. J. 133 (1–3) (2007) 173–186.
[19] S. Kapadia, W.K. Anderson, Sensitivity Analysis for Solid Oxide Fuel cells using a Three-Dimensional Numerical Model, J. Power Sources 189 (2) (2009) 1074–1082.
[20] N.P. Kikas, Laminar flow distribution in solar systems, Solar Energy 54 (4) (1995) 209–217.
[21] P.I. Shen, The effect of friction on flow distribution in dividing and combining flow manifolds, J. Fluids Eng. 114 (1992) 121–123, Transaction of ASME.
[22] M.K. Bassiouny, H. Martin, Flow distribution and pressure drop in plate heat exchanges. Part I. U-Type arrangement, Chem. Eng. Sci. 39 (4) (1984) 693–700.
[23] C.G. Speziale, B.A. Younis, S.A. Berger, Analysis and modelling of turbulent flow in an axially rotating pipe, J. Fluid Mech. 407 (2000) 1–26.
[24] J.Y. Wang, G.H. Priestman, Flow simulation in a complex fluidics using three turbulence models and unstructured grids, Int. J. Num. Methods Heat Fluid Flow 19 (3/4) (2009) 484–500.
[25] S. Jakirlic, K. Hanjalic, C. Tropea, Modeling rotating and swirling turbulent flows: a perpetual challenge, AIAA J. 40 (10) (2002) 1984–1996.
[26] J.Y. Wang, G.H. Priestman, J.R. Tippetts, Modelling of strongly swirling flows in a complex geometry using unstructured meshes, Int. J. Num. Methods Heat Fluid Flow 16 (8) (2006) 910–926.
[27] J.Y. Wang, Pressure drop and flow distribution in parallel-channel of configurations of fuel cell stacks: U-type arrangement, Int. J. Hydrogen Energy 33 (21) (2008) 6339–6350.
[28] J.Y. Wang, Pressure drop and flow distribution in parallel-channel of configurations of fuel cell stacks: Z-type arrangement, Int. J. Hydrogen Energy. 35 (2010) 5498–5550.
[29] J.Y. Wang, X.L. Ge, D.D. Wu, Progress of flow in manifolds, Adv. Mech. 28 (3) (1998) 392–401, in Chinese.
[30] J.S. McNown, Mechanics of manifold flow, Trans. ASCE 119 (1954) 1103–1142.

[31] A. Acrivos, B.D. Babcock, R.L. Pigford, Flow distributions in manifolds, Chem. Eng. Sci. 10 (1959) 112–124.
[32] A.V. Kulkarni, S.V. Badgandi, J.B. Joshi, Design of ring and spider type spargers for bubble column reactor: experimental measurements and CFD simulation of flow and weeping, Chem. Eng. Res. Design. 87 (2009) 1612–1630.
[33] R.J. Kee, P. Korada, K. Walters, M. Pavol, A generalized model of the flow distribution in channel networks of planar fuel cells, J. Power Sources 109 (2002) 148–159.
[34] S. Maharudrayya, S. Jayanti, A.P. Deshpande, Flow distribution and pressure drop in parallel-channel configurations of planar fuel cells, J. Power Sources 144 (2005) 94–106.
[35] J.Y. Wang, Comments on "Flow distribution in U-type layers or stacks of planar fuel cells", by W.H. Huang and Q.S. Zhu [J. Power Sources, 2008; 178: 353–362]. J. Power Sources. 190(2) (2009) 511–512.
[36] J.Y. Wang, M.C. Zhang, D.D. Wu, The effects of velocity distribution on the flow uniformity in the boiler's dividing header, Proc. Chin. Soc. Elec. Eng. 19 (5) (1999) 9–12, in Chinese.